Simple Topographic Parameter Reveals the Along-Trench Distribution of Frictional Properties on a Shallow Plate Boundary Fault

Hiroaki Koge (koge.h@aist.go.jp)
National Institute of Advanced Industrial Science and Technology https://orcid.org/0000-0002-8720-4975
Juichiro Ashi
University of Tokyo
Jin-Oh Park
University of Tokyo
Ayumu Miyakawa
National Institute of Advanced Industrial Science and Technology Geological Survey of Japan
Suguru Yabe
National Institute of Advanced Industrial Science and Technology Geological Survey of Japan

---

Full paper

Keywords: Subduction zone, Japan Trench, Critical taper model, Frictional variation, Accretionary wedge

Posted Date: October 13th, 2021

DOI: https://doi.org/10.21203/rs.3.rs-948355/v1

Version of Record: A version of this preprint was published at Earth, Planets and Space on April 21st, 2022. See the published version at https://doi.org/10.1186/s40623-022-01621-6.

Title page:

Title: Simple topographic parameter reveals the along-trench distribution of frictional properties on a shallow plate boundary fault

Author #1: Hiroaki Koge[1], koge.h@aist.go.jp ***as Corresponding author***

Author #2: Juichiro Ashi[2, 3], ashi@u-tokyo.aori.ac.jp

Author #3: Jin-Oh Park[2], jopark@aori.u-tokyo.ac.jp

Author #4: Ayumu Miyakawa[1], miyakawa-a@aist.go.jp

Author #5: Suguru Yabe[1], s.yabe@aist.go.jp

[1] Geological Survey of Japan, National Institute of Advanced Industrial Science and Technology, Central 7, 1-1-1 Higashi, Tsukuba, Ibaraki 305-8567, Japan

[2] Atmosphere and Ocean Research Institute, The University of Tokyo, 5-1-5 Kashiwanoha, Kashiwa-shi, Chiba 277-8564, Japan

[3] Department of Natural Environmental Studies Division of Environmental Studies, Graduate School of Frontier Sciences, The University of Tokyo, 5-1-5 Kashiwanoha, Kashiwa-shi, Chiba 277-8564, Japan

Abstract

The critical taper model of a sedimentary wedge best describes the first-order mechanics of a subduction zone wedge. The tapered wedge geometry, which is conventionally defined by two parameters, the slope angle and the basal dip angle, is responsible for the strength of a megathrust. By applying this theoretical model to subduction zones, fault frictional properties and earthquake occurrences can be compared among subduction zones, and within a single subduction zone, the spatial distribution or temporal change of fault strength can be investigated. The slope angle can be accurately estimated from bathymetry data, but the basal dip angle must be inferred from the subsurface structure, and it requires highly accurate depth-converted seismic reflection profiles. Thus, application of the critical taper model is often limited by a lack of a sufficient number of highly accurate profiles, and the spatial distribution of frictional coefficients must be inferred from relatively few data, generally less than a dozen points. To improve this situation, we revisited the theoretical formula of the critical taper model. We found that the effect of the décollement dip angle β on the critical taper model of a sedimentary wedge is negligible when the pore fluid pressure ratio is high or internal friction is small, conditions which are met in many subduction zones. Therefore, this finding allows frictional variation to be approximated by using only the slope angle variation obtained from the bathymetry. We applied this approximation to the Japan Trench as an example of this approximation, and were able to estimate the friction coefficient distribution on the shallow plate boundary fault from 71 data points. We found that the area where the friction coefficient was smaller than the mean corresponded to the segment where a large coseismic shallow rupture occurred during the 2011 Tohoku-oki earthquake (Mw 9.0). This result shows that by approximating tapered wedge geometry using a simple topographic parameter that can be obtained from existing global bathymetry, we can quickly estimate the distribution of frictional properties on a plate boundary fault along a trench and related seismic activity.

Keywords

Subduction zone, Japan Trench, Critical taper model, Frictional variation, Accretionary wedge

Main Text

1. Introduction

The first-order mechanics of a subduction zone wedge, a representative feature of a fold-and-thrust belt, can be clearly explained by the critical taper model (e.g., Dahlen 1990). This geomechanical model, which is based on the Mohr-Coulomb failure criterion, allows frictional properties on a plate boundary fault to be determined. This model is a key method for understanding megathrust earthquake mechanisms, because direct measurements of plate boundary fault strength are quite rare and require drilling into the deep décollement to obtain samples (e.g., Chester et al. 2013; Ujiie et al. 2013). According to this model, the tapered wedge geometry (slope angle α and basal dip angle β) is determined by the strengths of the wedge materials and the effective friction on the megathrust fault (μ_b') (Fig. 1). Thus, the critical taper model allows the geomechanical condition of a subduction wedge to be determined. This information can be used to compare geomechanical conditions among different subduction zones (e.g. Dahlen 1990) or to examine their spatial distribution within a single subduction zone (e.g., Fagereng 2011; Koge et al. 2014) or temporal changes along a single profile (e.g., Wang et al. 2010; Wang and Hu 2006). Slope angle α can be calculated from the bathymetry above the subduction wedge, which is typically observed by a multi-beam echosounder onboard a ship. Generally, the bathymetry is obtained with a vertical error on the order of several meters, so the accuracy with which α is determined is sufficient for characterizing the wedge geometry. However, the subsurface geometry parameter used in critical taper model calculations, namely, the basal dip angle β, requires further consideration. In a depth-converted profile of seismic reflection data, the depth to the plate boundary fault depends strongly on the velocity model used, and the accuracy of the depth-conversion process affects the value obtained for the topographic parameter β. Therefore, unless only highly accurate depth-converted profiles are used to calculate this critical taper model parameter, comparisons within and among wedges are likely to be unreliable. On a scale of several kilometers, pre-stack depth migration (PSDM) data or, at larger scale, a cross section of the velocity structure combined with refraction data can be used for accurate determination of β for the critical taper model. However, highly accurate PSDM data or seismic reflection profiles are often not available because they require more processing time and are more costly to process than a simple depth-converted profile. As a result, the number of accurate cross sections available for a critical taper analysis is often insufficient to reveal detailed along-strike variations of frictional properties in subduction zones.

2. Revisiting, validating, and improving critical taper theory

We first review formulations of Coulomb wedge/critical taper theory. All of the formulas are based on a non-cohesive wedge model, which assumes non-viscosity (Dahlen 1984). According to the Mohr-Coulomb failure criterion, $\tau = \sigma \cdot \tan\phi + C$, where τ is shear stress, σ is vertical stress, ϕ is the internal friction coefficient (also expressed as μ, the coefficient of internal friction averaged over the wedge), and C is the cohesion force. Because internal friction forces are proportional to vertical stress whereas cohesion forces are independent of vertical stress, the cohesion term can be neglected when considering huge geological structures with large σ. Thus, the noncohesive critical taper model is valid in the entire wedge.

Next, we theoretically verify the effect of the basal dip angle β on the calculation of effective friction μ_b' and show that the effect of β becomes small when the pore fluid pressure in the subduction zone is high. Hence, we propose that basal friction in subduction zones can be inferred from only the slope angle α determined from the bathymetry.

2.1 Revisiting critical taper theory: Overview of the critical taper model to obtain the effective coefficient of basal friction

Critical taper theory (Davis et al. 1983; Dahlen 1984; Lehner 1986) is a geomechanical model based on the Mohr-Coulomb failure criterion according to which the wedge geometry (α and β) is constrained by the balance between wedge strength and effective friction μ_b' (e.g., Adam and Reuther 2000).

In critical taper theory, we obtain μ_b' and the pore fluid pressure ratio (λ) in a wedge by drawing cross plots between λ and μ_b', as explained below (e.g., Adam and Reuther 2000; Wang and Hu 2006; Wang et al. 2010, 2019) (Fig. 2). In the critical taper theory formulation, the modified slope angle α' under subaerial conditions is formulated as

$$\alpha' = \tan^{-1}\left[\left(\frac{1-\rho_w/\rho}{1-\lambda}\right)\tan\alpha\right],$$

where α is a parameter obtained from the bathymetry/seismic profile, ρ is wedge sediment density, ρ_w is fluid density, and λ is the pore fluid pressure ratio. Then, the uniform angle between the most compressive principal stress axis σ_1 and the upper slope, ψ_0 (see Fig. 1), is calculated as,

$$\psi_0 = \frac{1}{2}\sin^{-1}\left(\frac{\sin\alpha'}{\sin\phi}\right) - \frac{1}{2}\alpha'$$

where ϕ is the angle of internal friction within the wedge. Because along-strike stresses are not considered in the critical taper model, the following simple geometric relation is applicable (Fig. 1):

$$\alpha + \beta = \psi_b - \psi_0$$

where ψ_b is the angle between σ_1 and the basal plane. Then, the effective coefficient of basal friction (μ_b') is obtained from the Mohr-Coulomb failure criterion τ and the stress balance of the basal condition as

$$\mu_b' = \frac{\tan 2\psi_b}{\csc\phi \sec 2\psi_b - 1}$$

To draw the limb of the cross plot between μ_b' and λ, we set λ to range between 0 and 1 (Fig. 2). The left limb of the critical state curve represents extensionally critical states, and the right limb represents compressively critical states. Then, under the assumption that λ is constant, we can obtain μ_b' from the intersection of λ and the critical state curve calculated earlier.

For example, if we assume the mean wedge parameters ρ = 2700 k/m^3, ρ_w = 1000 kg/m^3, internal friction angle φ = 34°, and λ = 0.88 (Lallemand et al. 1994) (Fig. 2), μ_b' can be determined from the intersection of λ = 0.88 with the critical state curve (Wang et al. 2019). Because the prism wedge in subduction zones should be in a constant compressively critical state just before failure, we focus on only the intersection with the right limb (representing compressively critical states). Thus, in this example, we obtain μ_b' = 0.06. For more details than are provided in this simple review, please see the cited studies.

2.2 Validation and improvement: Effects of the geometric parameters on μ_b'

In this study, we examined the sensitivity of the calculated μ_b' to the assumed α and β values to investigate how their accuracy affects the estimation of μ_b'. We used the mean subduction zone parameter values in the example described in section 2.1 and changed the values of α and β to see how μ_b' varied. The states of the frontal wedge with α = 5° and β = 1° or β = 5° are shown in Fig. 3A; in Fig. 3B both α and β are varied from 1° to 5°. We allowed β to range from 1° to 5° because that range includes the basal dip angle of most subduction zones (Lallemand et al. 1994; Wang et al. 2006). Here, since μ_b' cannot be determined when $\alpha = \beta = 0$, those results were removed.

As a result—and this might be a blind spot in previous research—we found that β has little influence on the estimation of μ_b' when the pore fluid pressure is high. The change in β (from 1° to 5°) dominantly accounts for the change in the width of the critical state curve (i.e., the angle between its limbs) between the two states illustrated in Fig. 3A. When λ is high, the intersection between λ and the right limb of the critical state curve is near the curve peak. Therefore, the change in the width due to a change in β has only a slight effect on μ_b'. In typical subduction zones, λ is high (~0.88) (Lallemand et al. 1994), so the effect of β should be regarded as a small one. Moreover, this finding is also favorable in terms of the accuracy of μ_b' obtained by applying the critical taper theory, because the seismic profile depth used to calculate β depends on the velocity model/structure of the seismic profile, which is often not obtained with high accuracy for reasons of time and money. Moreover, the number of available profiles is also important to obtain the distribution of frictional properties by applying critical taper theory. Thus, because β must be obtained from depth-converted profiles with low accuracy, the resulting error is large (Koge et al. 2014). In contrast, α can be determined with negligible error. The seafloor depth, which is used to calculate α, is mostly based on multibeam data and the sound velocity profile of seawater. These can be acquired with high accuracy by conductivity/temperature/depth (CTD) measuring systems, or by deploying expendable bathythermograph (XBT) or XCTD instruments, which generally have a vertical error on the order of several meters. Therefore, from this perspective, α can be obtained with negligible error. The more significant factor influencing the error of α is whether the obtained cross-section is aligned with the direction of maximum slope. However, if the deviation from the maximum slope direction is no more than 18°, the error in α will be less than 5% [see Additional file 1]. Therefore, α can reliably be obtained with high accuracy.

Under high pore fluid pressure conditions such as those in the mean subduction zone, the influence of β on the calculation of μ_b' should be small enough to ignore. Thus, the α variation can be used to approximate the relative along-trench variation of μ_b', and data accuracy is improved. In this first step, we considered as an example the mean conditions described in section 2.1 (Fig. 3B and Table 1).

The next step is to determine quantitatively under what conditions β can be ignored and the α–μ_b' approximation can be used. We used linear multiple regression analysis, a statistical method that can be used to predict the value of a variable (the response variable) from the value of two or more other variables (explanatory variables), to determine whether α or β affects the effective friction coefficient μ_b'. Here, we used α and β as explanatory variables and μ_b' as the response variable. We conducted this analysis with the stats-model API in Python (Seabold and Perktold 2010). The obtained regression equation is characterized by the coefficients of α and β (A and B, respectively) and the coefficient of multiple determination R^2. To evaluate the relative influence of α and β on μ_b', we also defined the parameter "weight of alpha" (WOA) = A/(A + B). For the mean subduction zone, we obtained R^2 = 0.99 and WOA = 77.50%. Thus, the goodness of fit of the regression equation, indicated by R^2, was high, and the contribution of α to μ_b' was also high at 77.50%.

Next, to determine whether β can be neglected in most subduction zones, we considered potential ranges of λ and φ in nature (λ = 0–1, φ = 20–39°), and then calculated WOA and R^2 for all combinations of λ and φ in these ranges (Fig. 4, raw data in Additional file 2). For example, using mean subduction wedge values of 21 representative trenches (Lallemand et al. 1994), (λ, φ) = (0.88, 34°), and WOA = 78.02%. Of course, in some exceptional subduction zones, such as at the Sunda and Makran trenches, λ is small (Wang and Hu 2006), so the appropriateness of the application of the α–$\mu b'$ approximation needs to be considered carefully. For more example, at the toe of the Japan Trench, Kimura et al. (2012) and Wang et al. (2019) assumed the following parameters: (λ, φ) = (0.8, 21.8°) and (λ, φ) = (0.95, 36°), respectively. Given that under these conditions, WOA = 79.86% and 88.54%, respectively (Fig. 4), in the toe of the Japan Trench, the frictional variation in the wedge can be roughly regarded as determined by α alone. Therefore, if the WOA of the targeted subduction zone is sufficiently high, frictional conditions along the plate interface can be obtained by using α alone.

3. Application example of the α–μ_b' approximation to the Japan Trench

Through our review and verification of the critical taper model, we found that β can be ignored not only when λ is high but also when WOA is high, owing to either high λ or low φ (Fig. 4). Thus, in our approximation, the spatial variation in the slope angle α is an indicator of the variation in the effective basal friction μ_b', and, we can use only bathymetry data to obtain the distribution of the friction coefficient within a single subduction zone. Here, we apply this approximation to the Japan Trench. The Japan Trench is suitable for the application of this method because, as shown in section 2.2, WOA is high in the toe portion of the wedge and the friction coefficient along the plate interface can thus be estimated from only α, as well as because a rupture occurred near the trench axis during the 2011 Tohoku-Oki earthquake (Mw 9.0). Therefore, by comparing the distribution of α which should reflect that of μ_b' in Japan Trench, the question of why such coseismic rupture occurred in specific area can be addressed.

To apply our approximation model to the Japan Trench, we used the 250-m grid data of Kishimoto (2000), focusing on the shallow portion within a horizontal distance of 25 km from the trench axis, and obtained the distribution of α, interpreted as the relative friction distribution, on the shallow megathrust (Fig. 5, Table 2). As a result, using bathymetric profiles and slope angles obtained by modifying GMT/MATLAB code as described by Wessel and Luis (2017), we accurately obtained the along-strike distribution of μ_b' on the shallow plate boundary fault at 71 points (instead of at only a dozen points or less, as is typical in applications of critical taper theory).

The low-α segment (low-μ_b' segment), located at approximately 36°–39°N, corresponds to the coseismic slip distribution of the 2011 Tohoku-Oki earthquake (Chester et al. 2013). This result suggests large fault rupture in the low-α segment have occurred, causing the slip to propagate to the shallow portion of the plate boundary fault, because of the low friction there. And it lead to the huge tsunami (e.g. Ide et al., 2011). In contrast, the south and north ends of the coseismic slip zone are relatively high-friction areas. As a result, the slip could not propagate to these other segments because the high friction acted as a barrier. Therefore, the low friction in the shallow area can be considered to be the cause of the huge tsunami. In addition, the low-α segment identified here approximately corresponds to the central segment along the Japan Trench (~37°–39°N) inferred from the distribution of seismic activity detected by the S-net ocean-bottom seismograph network (Nishikawa et al. 2019).

Low-friction conditions might prevail generally along the Japan Trench margin, except in regions of high friction caused by the recent subduction of a seamount (Mochizuki et al. 2008) or the presence of petit-spot volcanoes (Hirano et al. 2006). Because μ_b' depends on both λ and φ, it is not possible to determine whether variation in

α (i.e., relative μ_b') is due to a change in physical properties or to a change in pore fluid pressure. Although here we cannot separate the effect of physical properties from that of pore fluid pressure on α, both effects are reflected in the strength of the megathrust.

4. Conclusion

We presented an approach to the application of the critical taper model that, intriguingly, has the potential to advance our ability to characterize basal friction along the shallow plate interface in subduction zones. First, we reviewed the critical taper model formulas used for calculating the effective coefficient of basal friction μ_b'. We found that in most subduction zones, the effect of β on basal friction can be regarded as slight, especially when WOA is high, which occurs when λ is high or φ is low. The spatial variation of α can be easily obtained with high accuracy from bathymetry data obtained by multi-beam observation. Even in areas where observation is difficult, there are ETOPO1 (Amante and Eakins 2009) or other global datasets obtained by the satellites, most of which are free to access and also have a vertical error of only a few tens of meters (Varga and Bašić 2015). Note that these global data set based on satellite observations, so the vertical error order is a little larger. Therefore, by applying this approximation, the frictional distribution in subduction zones can now easily be evaluated.

The approximated critical taper model proposed in this study can improve the resolution of the along-trench distribution of μ_b' determined on a shallow megathrust. By applying our approach to the Japan Trench, we showed that the seafloor slope angle (relative μ_b') is systematically smaller within the area of large coseismic shallow slip during the 2011 Tohoku-Oki earthquake than it is in areas to the south and north, where little coseismic slip has been imaged. In the future, a global study is needed to examine the correlation between frictional conditions along the plate interface as revealed by the seafloor topography and seismicity and improve our understanding of the connection between earthquake physics and tectonics. Our critical taper results are given in Additional file 3, attached. By referring to this file, the coefficient of effective friction on the plate boundary fault can be determined if the geomechanical parameters λ, φ, α, and β of the subduction zone are known.

Declarations: *Not applicable*

Consent for publication: *Not applicable*

Availability of data and materials

All data are available in the main text or in the supplementary materials.

Competing interests

Authors declare no competing interests.

Funding

HK was supported by JSPS KAKENHI Grant Number JP17K05687. JA and JP are supported by JSPS KAKENHI Grant Number JP18H03732. AM is supported by JSPS KAKENHI (Grant-in-Aid for Scientific Research on Innovative Areas) Grant Number JP17H05321. SY is supported by JSPS KAKENHI Grant Number 21H01189.

Authors' contributions

H. Koge mainly contributed to conceptualization, data curation, methodology, visualization, and writing of the original draft. J. Ashi and J.-O. Park conducted fundamental research on the geological settings of subduction zones and contributed to the discussion. A. Miyakawa and S.

Yabe contributed to the methodology and discussion. All authors helped to write, review, and edit the paper.

Acknowledgements and Endnotes

A. Yamaguchi, G. Kimura, and A. Noda provided advice on fundamental research about frontal prisms. We acknowledge anonymous reviewers for their thoughtful reviews.

References

Adam J, & Reuther C D (2000) Crustal dynamics and active fault mechanics during subduction erosion. Application of frictional wedge analysis on to the North Chilean Forearc. Tectonophysics, 321, 297–325. doi:10.1016/S0040-1951(00)00074-3

Amante C, & Eakins B W (2009) ETOPO1 1 Arc-Minute Global Relief Model: Procedures, Data Sources and Analysis. NOAA Technical Memorandum NESDIS NGDC-24, 19. doi:10.1594/PANGAEA.769615

Chester F M, Rowe C, Ujiie K, *et al.* (2013) Structure and composition of the plate-boundary slip zone for the 2011 Tohoku-Oki earthquake. Science, 342, 1208–

1211. doi:10.1126/science.1243719

Dahlen F A (1984) Noncohesive Critical Coulomb Wedges: an Exact Solution. Journal of Geophysical Research, 89, 10125–10133. doi:10.1029/JB089iB12p10125

Dahlen F (1990) Critical Taper Model Of Fold-And-Thrust Belts And Accretionary Wedges. Annual Review of Earth and Planetary Sciences, 18, 55–99. doi:10.1146/annurev.earth.18.1.55

Davis D, Suppe J, & Dahlen F A (1983) Mechanics of fold-and- thrust belts and accretionary wedges. Journal of Geophysical Research, 88, 1153–1172. doi:10.1029/JB088iB02p01153

Fagereng A (2011) Wedge geometry, mechanical strength, and interseismic coupling of the Hikurangi subduction thrust, New Zealand. Tectonophysics, 507, 26–30. doi:10.1016/j.tecto.2011.05.004

Hirano N, Takahashi E, Yamamoto J, *et al.* (2006) Volcanism in response to plate flexure. Science, 313, 1426–1428. doi:10.1126/science.1128235

Ide S, Baltay A, Beroza, GC (2011) Shallow dynamic overshoot and energetic deep rupture in the 2011 Mw 9.0 Tohoku-Oki earthquake. Science, 332(6036), 1426-1429.

doi:10.1126/science.1207020

Kimura G, Hina S, Hamada Y, *et al.* (2012) Runaway slip to the trench due to rupture of highly pressurized megathrust beneath the middle trench slope: The tsunamigenesis of the 2011 Tohoku earthquake off the east coast of northern Japan. Earth and Planetary Science Letters, 339–340, 32–45. doi:10.1016/j.epsl.2012.04.002

Kishimoto K (2000) Combined Bathymetric and Topographic Mesh Data: Japan 250m Grid. Open File Rep. 353, 1-CD-ROM.

Koge H, Hamahashi M, Kimura G, *et al.* (2014) Friction properties of the plate boundary megathrust beneath the frontal wedge near the Japan Trench: An inference from topographic variation Multidisciplinary. Earth, Planets and Space, 66, 1–10. doi:10.1186/s40623-014-0153-3

Lallemand S E, Schnürle P, & Malavieille J (1994) Coulomb theory applied to accretionary and nonaccretionary wedges: Possible causes for tectonic erosion and/or frontal accretion. Journal of Geophysical Research: Solid Earth, 99, 12033–12055. doi:10.1029/94jb00124

Lehner F K (1986) Comments on “Noncohesive critical Coulomb wedges: An exact solution" by F. A. Dahlen. Journal of Geophysical Research, 91, 793. doi:10.1029/jb091ib01p00793

Mochizuki K, Yamada T, Shinohara M, *et al.* (2008) Weak interplate coupling by seamounts and repeating M ~ 7 earthquakes. Science, 321, 1194–1197. doi:10.1126/science.1160250

Nishikawa T, Matsuzawa T, Ohta K, *et al.* (2019) The slow earthquake spectrum in the Japan Trench illuminated by the S-net seafloor observatories. Science, 365, 808–813. doi:10.1126/science.aax5618

Seabold, Skipper, Josef Perktold. "statsmodels: Econometric and statistical modeling with python." Proceedings of the 9th Python in Science Conference. 2010., https://www.statsmodels.org/stable/index.html

Ujiie K, Tanaka H, Saito T, Tsutsumi A, Mori J, Kameda J, Brodsky E, Chester FM, Eguchi N, Toczko S, Expedition 343 and 343T Scientists (2013) Low coseismic shear stress on the Tohoku-Oki megathrust determined from laboratory experiments. Science, 342, 1211–1214. doi:10.1126/science.1243485

Varga M, & Bašić T (2015) Accuracy validation and comparison of global digital elevation models over Croatia. International Journal of Remote Sensing, 36, 170–189. doi:10.1080/01431161.2014.994720

Wang K, & Hu Y (2006) Accretionary prisms in subduction earthquake cycles: The theory of dynamic Coulomb wedge. Journal of Geophysical Research: Solid Earth, 111, . doi:10.1029/2005JB004094

Wang K, Brown L, & Hu Y (2019) Stable Forearc Stressed by a Weak Megathrust : Mechanical and Geodynamic Implications of Stress Changes Caused by the M = 9 Tohoku - Oki Earthquake Journal of Geophysical Research : Solid Earth, 6179–6194. doi:10.1029/2018JB017043

Wang K, Hu Y, von Huene R, *et al.* (2010) Interplate earthquakes as a driver of shallow subduction erosion. Geology, 38, 431–434. doi:10.1130/G30597.1

Wessel P, Luis J F (2017) The GMT/MATLAB Toolbox. Geochemistry, Geophysics, Geosystems, 18, 811–823. doi:10.1002/2016GC006723

Figure legends

Figure 1. Schematic illustration of the critical taper model. A Cross section of the forearc wedge in the Japan Trench (modified from Kimura et al. 2012). α: slope angle, β: basal dip angle β, μ_b' effective friction on the megathrust fault. The frontal wedge area is between the blue broken lines. **B** Diagram showing the self-similar growth of a bulldozer wedge (modified from Dahlen 1990).

Figure 2. Cross plot between the pore fluid pressure ratio λ and basal friction μ_b' in the wedge. All extensionally critical states form the left limb of the critical state curve, and all compressively critical states form the right limb. The stable region is under the curve (white). The straight-line intersecting the critical state curve represents constant λ.

Figure 3. Considering the weight of *β*. A The mechanically critical value of a frontal wedge is controlled by the fluid pressure ratio within the prism (λ) and the effective basal friction (μ_b'). The solid and broken lines represent the critical state curve for

different values of β. **B** Variation in μ_b' when α and β are varied from 1° to 5°, assuming mean subduction wedge conditions.

Figure 4. Heat map for weight of alpha (WOA). The closer WOA is to 100%, the more friction can be considered in terms of seafloor topography alone, because μ_b' can be determined from α alone. Conditions in the Japan Trench according to Kimura et al. (2012) and Wang et al. (2019) are shown by the two white squares.

Figure 5. Comparison of the spatial variation of slope angle α in the Japan Trench and the coseismic slip distribution. **A** Compiled coseismic slip along the Japan Trench (red contours). The epicenter of the Tohoku-Oki earthquake is shown by a yellow star, and the red lines show the positions of bathymetric profiles used to obtain α. **B** The distribution of α along the Japan Trench. The red area corresponds to the coseismic slip area in the map in **A** (Chester et al. 2013). The orange bar indicates the peak of the α distribution histogram.

Tables

Table 1. Values of μ_b' obtained by varying α and β from 1° to 5°. The left table was calculated by assuming mean subduction wedge conditions. The right table was calculated using conditions in the outer wedge of the Japan Trench.

Table 2 Slopes measured along bathymetric profiles on the landward side of the Japan Trench.

Additional files

Additional file 1: Supplemental text.pdf

Additional file 2: result_ols.csv; raw data for WOA plot (Fig. 4)

Additional file 3: result_ct.csv; raw results for critical taper parameters.

Figures

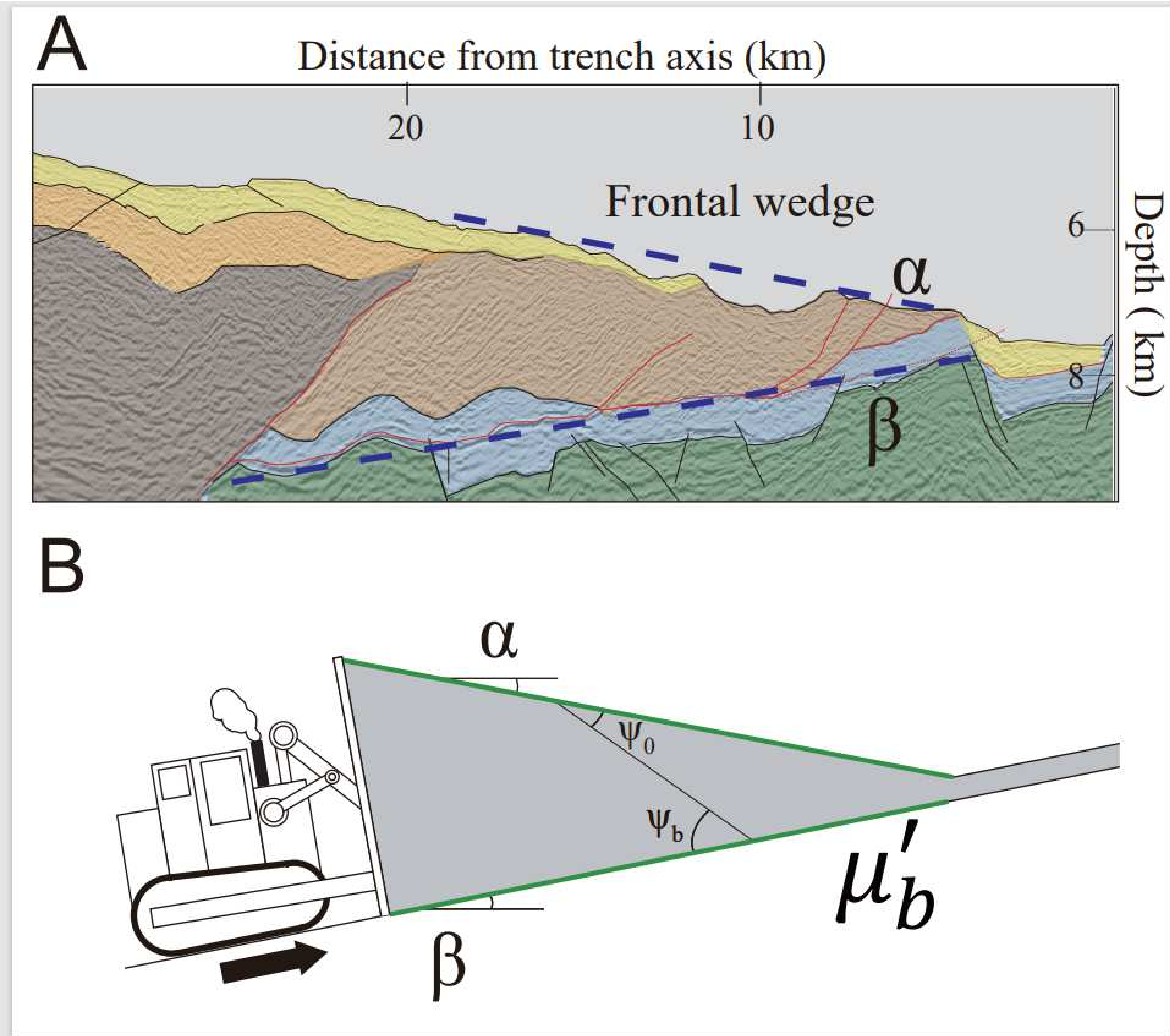

Figure 1

Schematic illustration of the critical taper model. A Cross section of the forearc wedge in the Japan Trench (modified from Kimura et al. 2012). α: slope angle, β: basal dip angle β, μb' effective friction on the megathrust fault. The frontal wedge area is between the blue broken lines. B Diagram showing the self-similar growth of a bulldozer wedge (modified from Dahlen 1990).

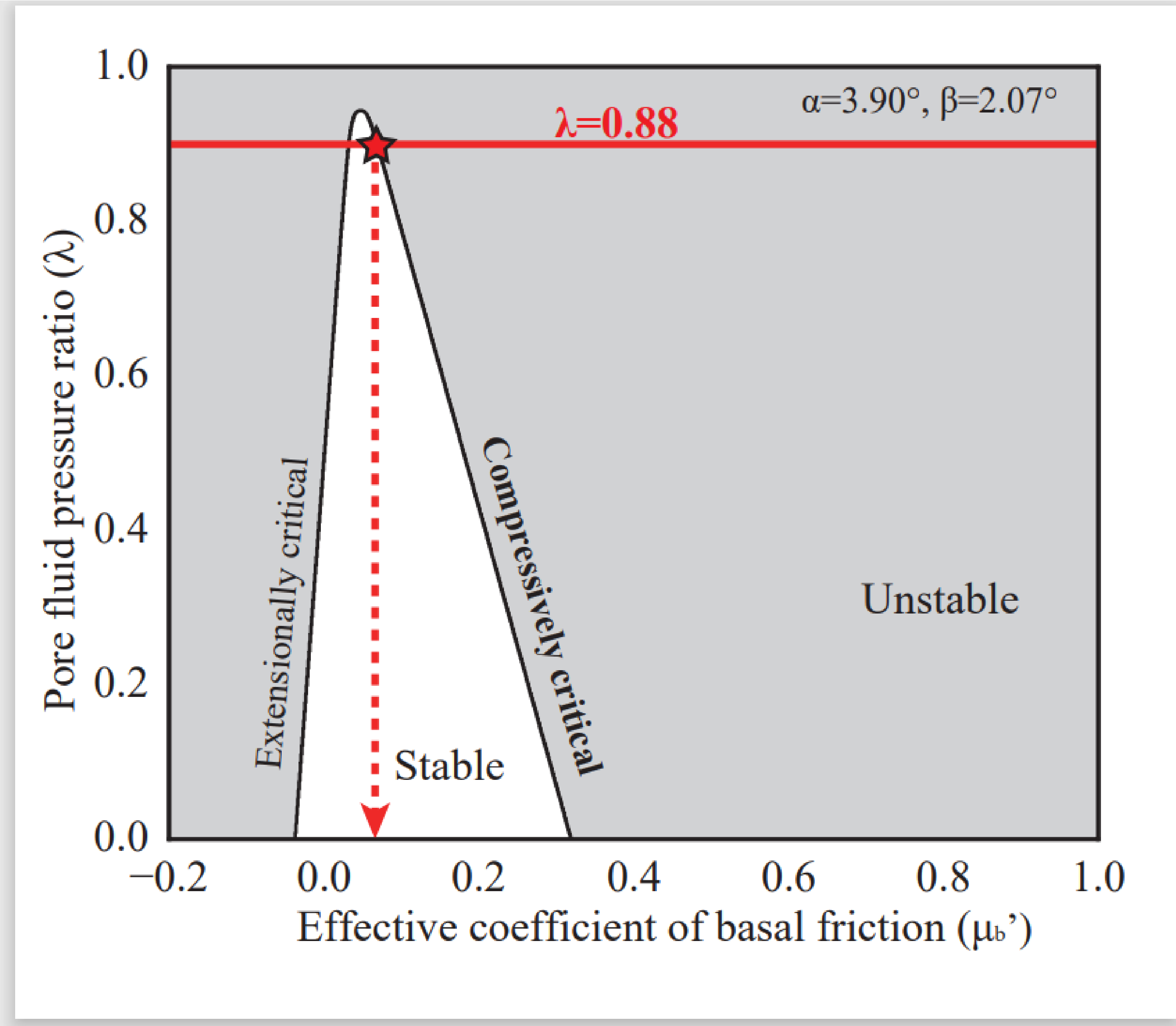

Figure 2

Cross plot between the pore fluid pressure ratio λ and basal friction μb' in the wedge. All extensionally critical states form the left limb of the critical state curve, and all compressively critical states form the right limb. The stable region is under the curve (white). The straight-line intersecting the critical state curve represents constant λ.

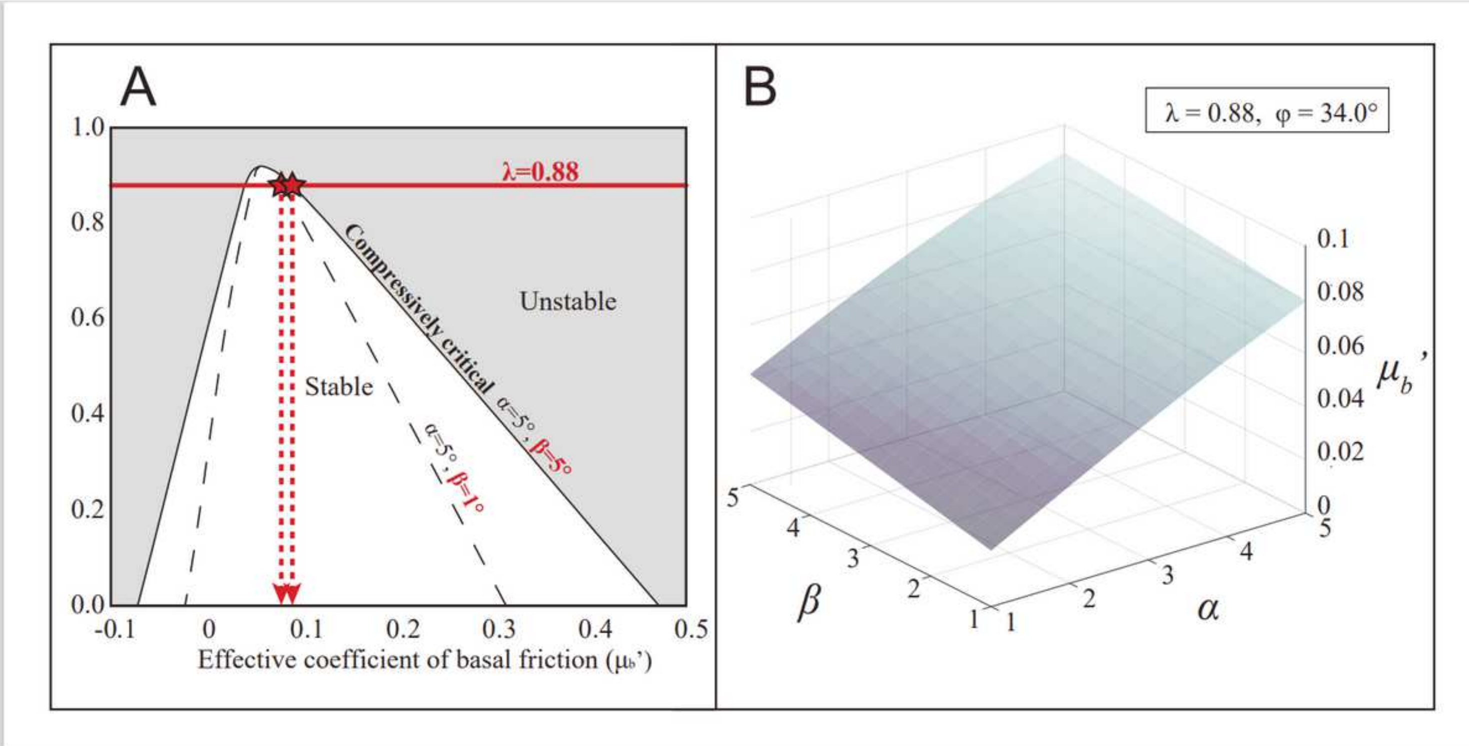

Figure 3

Considering the weight of β. A The mechanically critical value of a frontal wedge is controlled by the fluid pressure ratio within the prism (λ) and the effective basal friction (μb'). The solid and broken lines represent the critical state curve for different values of β. B Variation in μb' when α and β are varied from 1° to 5°, assuming mean subduction wedge conditions.

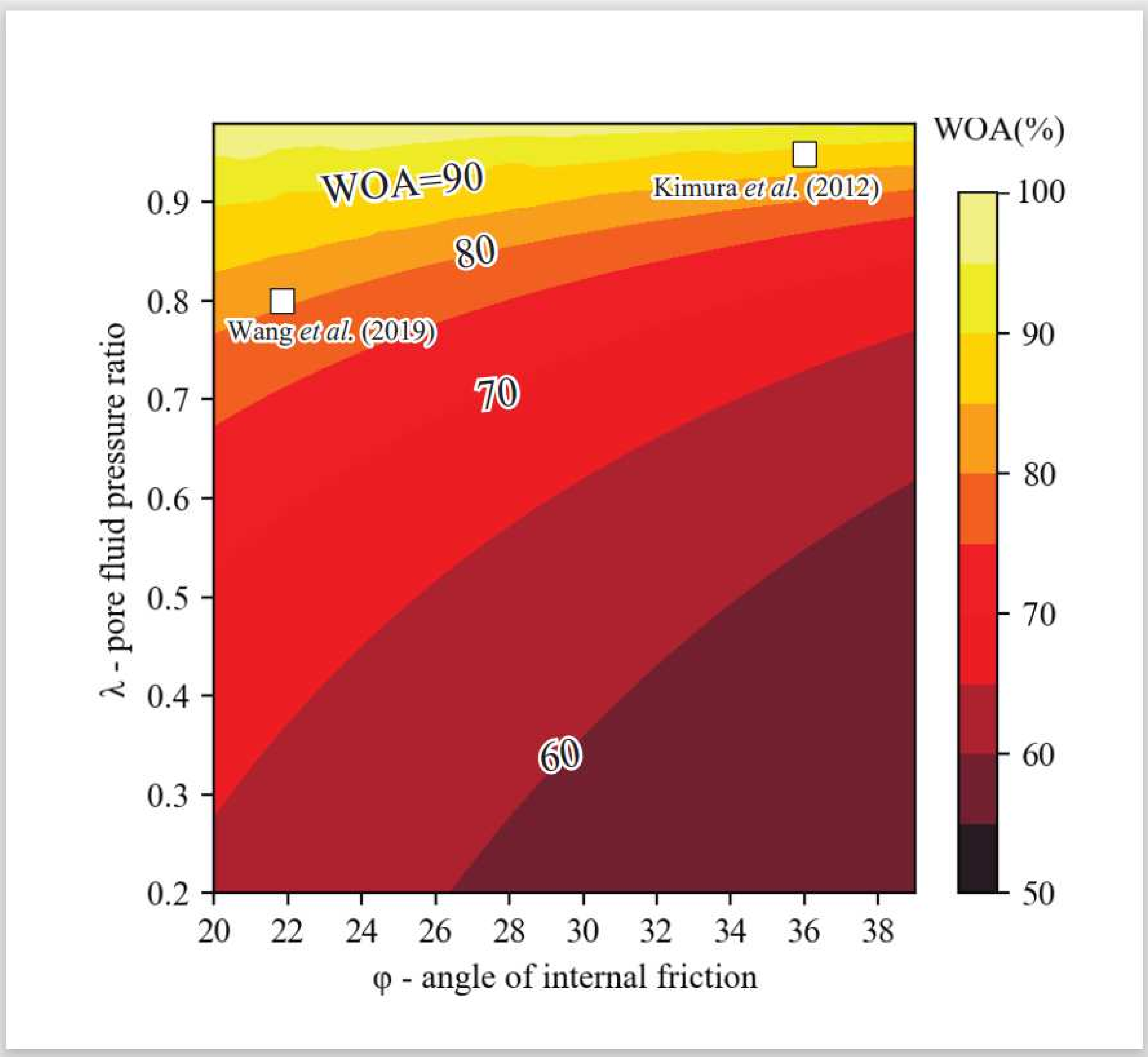

Figure 4

Heat map for weight of alpha (WOA). The closer WOA is to 100%, the more friction can be considered in terms of seafloor topography alone, because μb' can be determined from α alone. Conditions in the Japan Trench according to Kimura et al. (2012) and Wang et al. (2019) are shown by the two white squares.

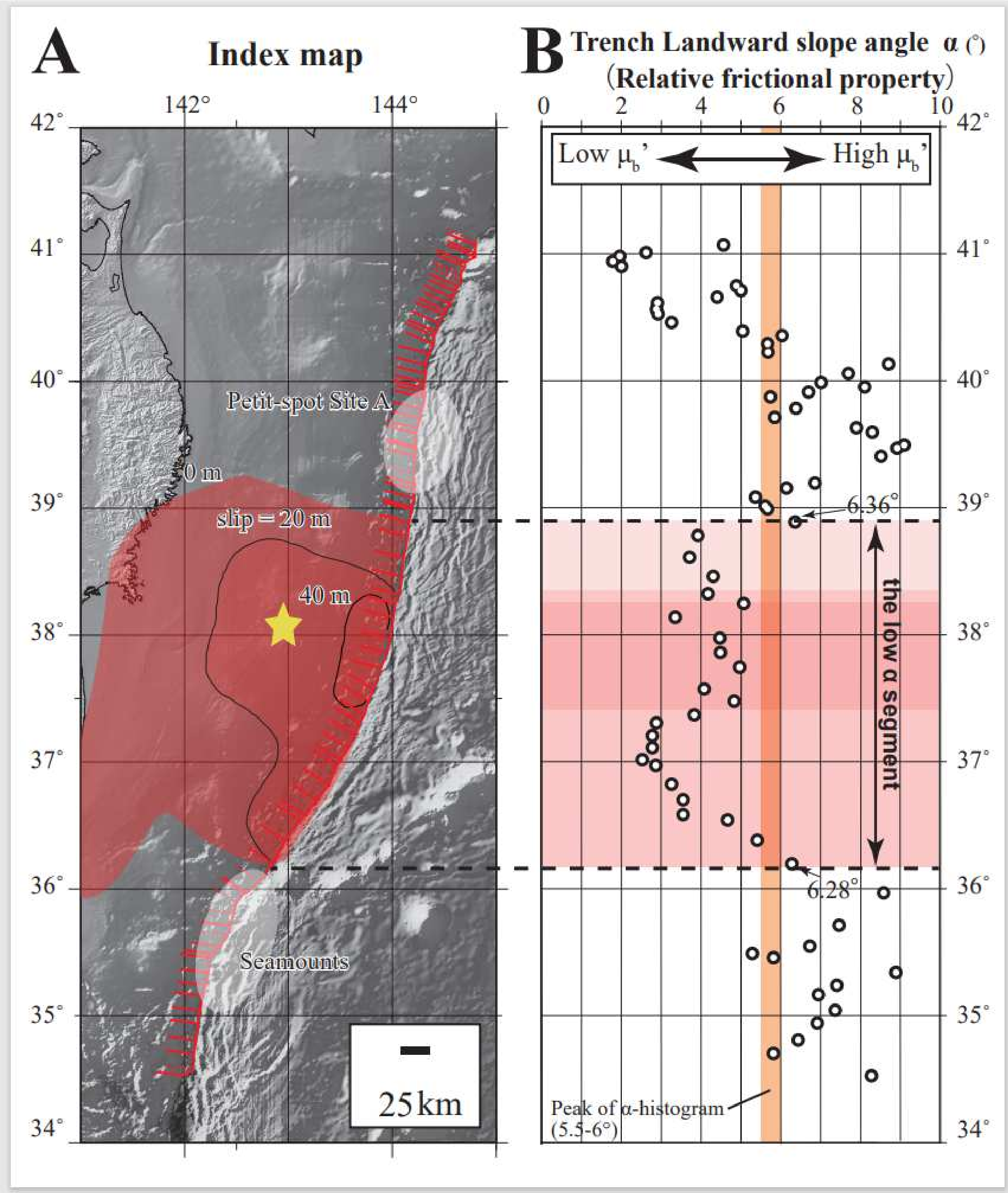

Figure 5

Comparison of the spatial variation of slope angle α in the Japan Trench and the coseismic slip distribution. A Compiled coseismic slip along the Japan Trench (red contours). The epicenter of the Tohoku-Oki earthquake is shown by a yellow star, and the red lines show the positions of bathymetric profiles used to obtain α. B The distribution of α along the Japan Trench. The red area corresponds to the coseismic slip area in the map in A (Chester et al. 2013). The orange bar indicates the peak of the α distribution histogram.

Supplementary Files

This is a list of supplementary files associated with this preprint. Click to download.

- FigureABSTRUCT.jpg
- Supplementarytext.pdf
- resultols.csv
- resultct.csv